ECS Transactions, 50 (3) 223-228 (2012)
10.1149/05003.0223ecst ©The Electrochemical Society

Degradation Study of Single and Double-Heterojunction InAlN/GaN HEMTs by Two-Dimensional Simulation

V. Palankovski[a], G. Donnarumma[a], and J. Kuzmik[a,b]

[a] AMADEA Group, Inst. for Microelectronics, TU Wien, 1040 Vienna, Austria
[b] Inst. of Elec. Engineering, Slovak Academy of Sciences, 84104 Bratislava, Slovakia

We study the concept of double-heterostructure quantum well (DHQW) InAlN/GaN/AlGaN high electron mobility transistor (HEMT) for higher device robustness and less degradation. Physics-based device simulation proves that the back barrier blocks the carrier injection into the device buffer. However, the energy of the injected electrons in the buffer is higher for any quantum well design in InAlN/GaN than in AlGaN/GaN HEMTs. This energy may be sufficient for releasing hydrogen from GaN point defects.

Introduction

InAlN/GaN HEMTs are an excellent alternative to AlGaN/GaN HEMTs for ultra high-frequency [1, 2] and power [3] applications. In this work, we address possible hot electron degradation of the buffer layer, which is one of the most critical issues for InAlN/GaN HEMTs [4]. For AlGaN/GaN HEMTs, it was shown that electrical stress at drain voltage V_{DS} = 20V and gate voltage V_{GS} close to the pinch-off can reduce the transconductance and degrade the GaN buffer. The effect was explained by the high electric field giving sufficient energy (0.72eV-3.55eV) to electrons to dehydrogenate point defects in the buffer [5, 6]. The changes are irreversible and can lead to a shift in the threshold voltage and to degraded channel mobility. A better confinement of electrons in the AlGaN/GaN HEMT channel and a reduced rate of carrier injection in the GaN buffer were observed for the double-heterostructure quantum well (DHQW) system by applying an AlGaN back barrier [7, 8]. Consequently, a lower sub-threshold drain leakage [7, 8] and a reduced trapping in the buffer [8] could be obtained. The AlGaN back barrier has also been tested in InAlN/GaN HEMTs, resulting in an improved device RF performance and reduced short-channel effects [9].

Device Description and Simulation Setup

In recent work, $In_{0.17}Al_{0.83}N$(14nm)/GaN(1.2μm) single quantum well (SQW) and novel $In_{0.17}Al_{0.83}N$(14nm)/GaN(50nm)/$Al_{0.04}Ga_{0.96}N$(310nm)/GaN(1.2μm) DHQW HEMT structures were degraded by applying off-state stress [10]. Three orders of magnitude lower gate and drain off-state leakage currents were observed in DHQW compared to those of SQW HEMTs [10]. The gate length is 250nm, and the gate-to-drain distance is 1.5μm. Our two-dimensional device simulator Minimos-NT, which is well-suited for numerical analysis of GaN HEMTs [11], is used to evaluate hot-electron injection effects in the buffer. The hydrodynamic transport model offers maximum accuracy combined with computational efficiency for sub-halfmicron GaN transistors.

Self-heating effects are accounted for by the lattice heat flow equation. A system of four partial differential equations: Poisson, current continuity and energy balance for electrons, and the lattice heat flow equations, is solved self-consistently. These four differential equations have material-specific parameters, such as the bandgap energy, electron mobility, thermal conductivity, etc. The dependence of these parameters on temperature, carrier energy, etc. is described by proper physics-based models [11].

Simulation Results

Very good agreement between measured and simulated transfer characteristics for both SQW and DHQW HEMTs is obtained (see Fig.1, virgin devices) by using polarization charge density $2.6\times10^{13}\text{cm}^{-2}$ at the channel/barrier interface and $-1.2\times10^{13}\text{cm}^{-2}$ at the barrier surface, which corresponds to a surface potential of ~1.4eV. Source and drain Ohmic contact resistivity ~0.4Ωmm, Schottky contact barrier height of ~1.4eV, and low-field electron mobility $560\text{cm}^2/\text{Vs}$ are assumed. For the DHQW structure, additional polarization charges with density $1.5\times10^{12}\text{cm}^{-2}$ and $-1.5\times10^{12}\text{cm}^{-2}$, respectively, at the bottom and at the top interfaces of the AlGaN layer are accounted for. By using these assumptions and the same concise set of models and model parameters, quite good agreement is achieved also for the output characteristics of both structures (see Fig.2, virgin devices). We note that a kink effect is observed in the measured output characteristics which accounts for some deviation compared with the simulation.

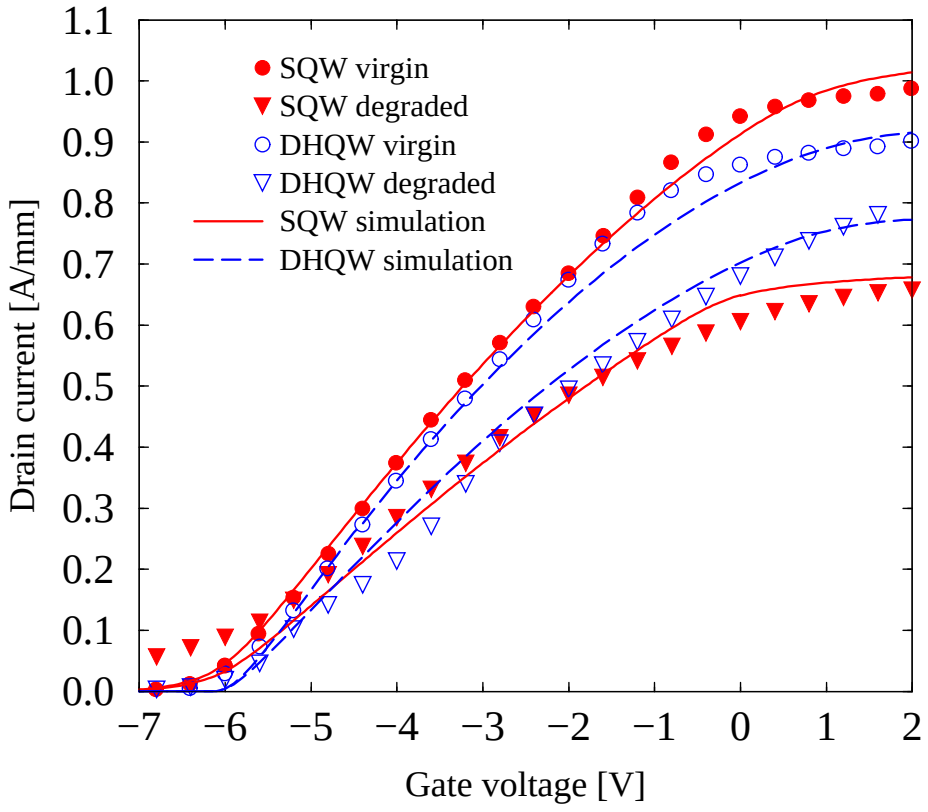

Figure 1. Comparison of measured (symbols) and simulated (lines) transfer characteristics of SQW (filled symbols) and DHQW (open symbols) HEMTs before (circles) and after (triangles) degradation.

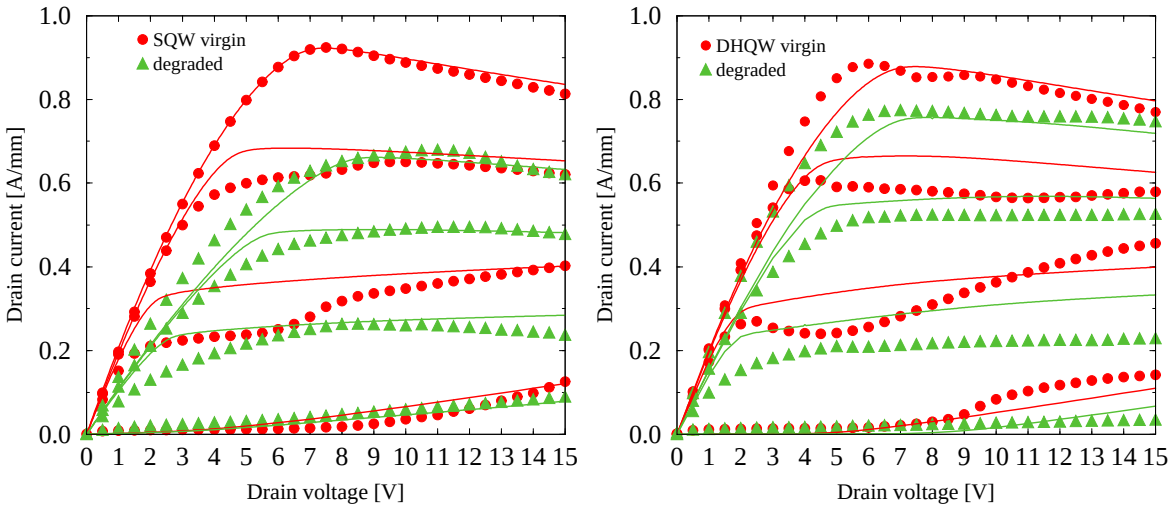

Figure 2. Comparison of measured (symbols) and simulated (lines) output characteristics of SQW (left) and DHQW (right) HEMTs before (circles) and after (triangles) degradation.

As can be seen from Figs.1 and 2 (degraded devices), it was experimentally observed that the DQHW HEMT is less vulnerable to degradation [10]. Simulation results for the experimental SQW and DHQW $In_{0.17}Al_{0.83}N$/GaN HEMTs and for a hypothetical $Al_{0.22}Ga_{0.78}N$/GaN HEMT were compared. 22nm $Al_{0.22}Ga_{0.78}N$ layer thickness was chosen, so that all devices share the same geometries and threshold voltage of –6.8V.

For example, Fig.3 shows the electron temperature (T_n) distribution near the drain side of the gate in the SQW and DHQW HEMTs. Our results for V_{GS} = –8V and V_{DS} = 20V indicate much higher energies of electrons injected in the buffer layer of the InAlN/GaN than in AlGaN/GaN HEMTs. In particular, the "hot spot" in the buffer of the AlGaN/GaN HEMT reaches T_n~7000K (corresponding to ~0.95eV) in comparison with T_n ~20000K for the InAlN/GaN HEMTs (see Fig.4). The indicated T_n in AlGaN/GaN corresponds only to the onset of a possible dehydrogenation of defects, which has a minimum required energy of ~0.7eV. On the other hand, hot electrons in the InAlN/GaN HEMT buffer seem to have sufficient energy for releasing H^+ atoms, i.e. it is more vulnerable to degradation. The higher T_n is due to the higher polarization fields in InAlN/GaN than in AlGaN/GaN HEMTs, which require the application of a sufficient gate bias to deplete the channel. The resulting vertical electric field in InAlN/GaN HEMTs in off-state deflects the channel electrons with higher energies in the buffer. Furthermore, we compared SQW and DHQW InAlN/GaN HEMTs (see Fig.4). The peak T_n is not much affected by the presence of the AlGaN back barrier, however, as indicated by the lateral cross sections (Fig.4), there is a much lower concentration of injected electrons in the DHQW than in the SQW HEMT. This may explain the higher stability of the DHQW InAlN/GaN HEMTs. Moreover, besides the blocking effect of the back barrier on the injection of hot electrons, the negative polarization charges at the GaN/AlGaN raise the conduction band in the GaN channel, which increases the T_n required for the dehydrogenation of point defects [12].

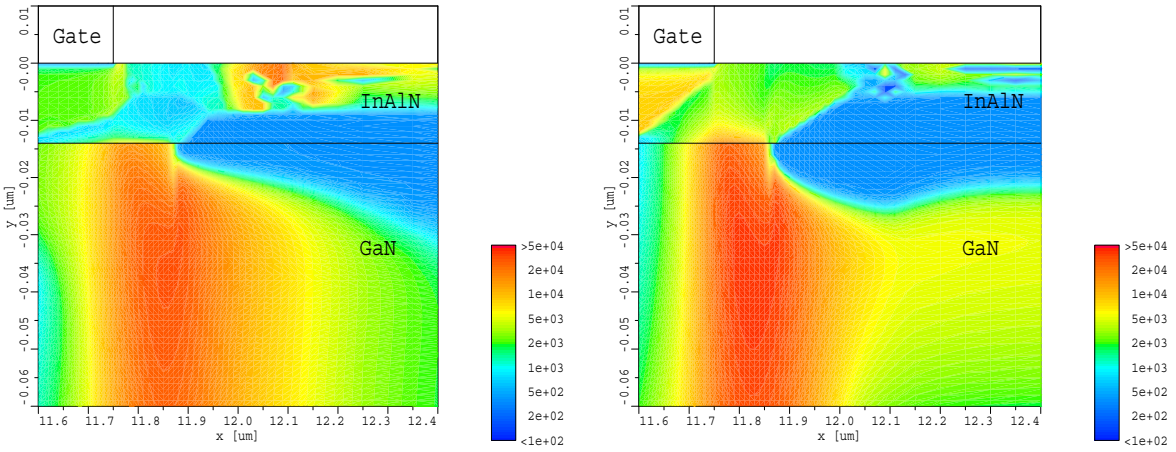

Figure 3. Calculated two-dimensional electron temperature maps [K] at the drain side of the gate in SQW (left) and DHQW (right) HEMTs.

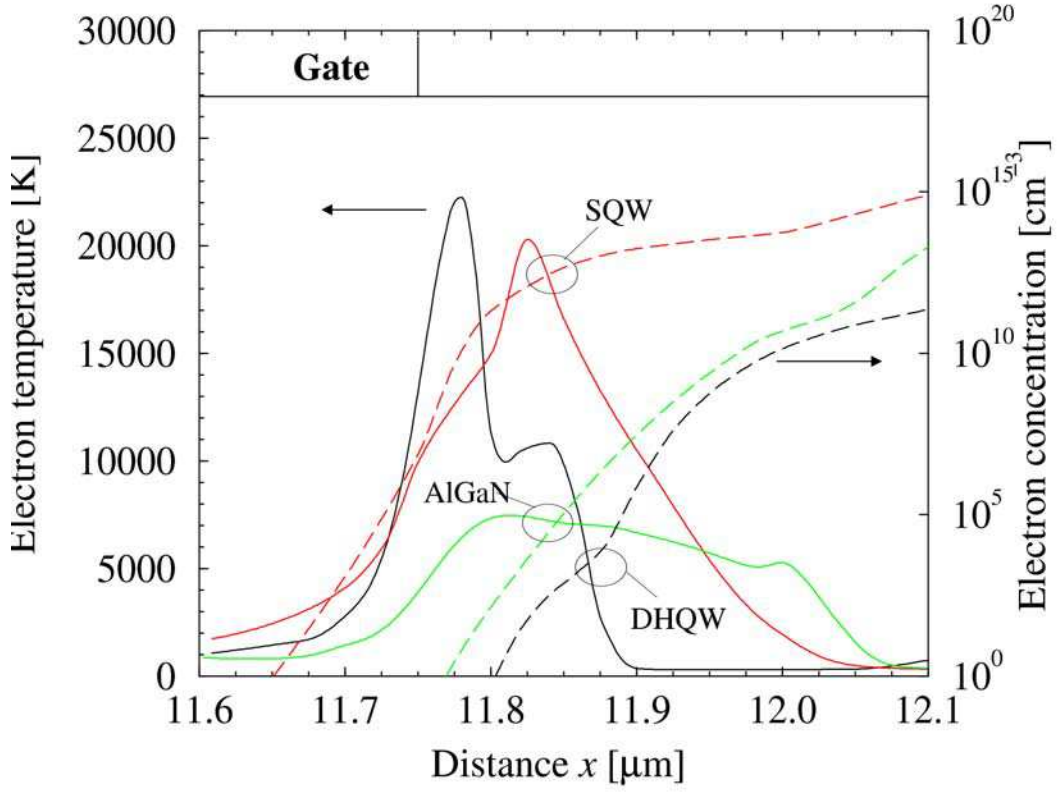

Figure 4. Cross sections of the electron concentration (dashed lines) and temperature (solid lines) in AlGaN/GaN (green color) SQW, InAlN/GaN SQW (red), and DHQW (black) HEMTs at $V_{GS} = -8$V and $V_{DS} = 20$V. The position of the cross sections along the GaN channel at a distance 11nm from the QW.

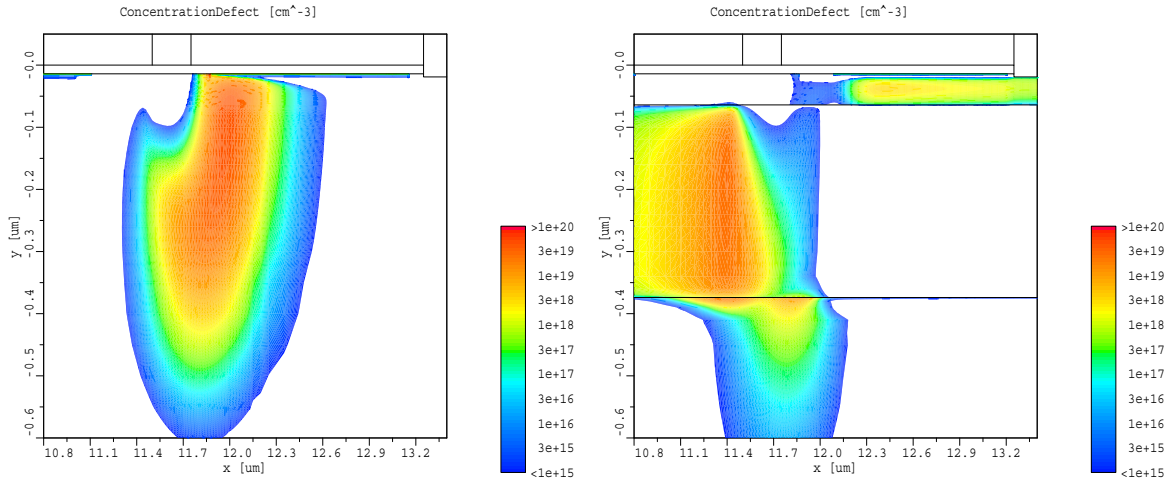

Figure 5. Distribution of defects due to hot-electron degradation in SQW (left) and DHQW (right) HEMTs. Defect densities are arbitrary and depend of the parameters (activation energy) of the particular defect.

We employ a simple degradation model, which links the product of electron concentration and an exponential function of electron energy in the stress condition of $V_{GS} = -8V$ and $V_{DS} = 20V$ to the density of resulting defects. In turn, device simulations, which account for these defects, are performed and compared to experimental characteristics of degraded structures. Fig.5 shows the distribution of defects for both structures. Device simulation results using these distributions give quite good agreement with the measurement data shown in Figs. 1 and 2 (degraded curves). The most notable difference in the distributions of defects is that while in SQW structure the defects occur close to the QW, this is not the case for the DHQW device.

Acknowledgments

This work was supported by the Austrian Science Funds FWF, START Project No.Y247-N13. Slovak R&D Agency Project No.APVV-0104-10 is also acknowledged.

References

1. D.S. Lee, J.W. Chung, H. Wang, X. Gao, S. Guo, P. Fay, and T. Palacios, *IEEE Elec. Dev. Lett.* **32**(6), 755, (2011).
2. H. Sun, A.R. Alt, H. Benedickter, E. Feltin, J.-F. Carlin, M. Gonschorek, N.R. Grandjean, and C.R. Bolognesi, *IEEE Elec. Dev. Lett.* **31**(9), 957, (2010).
3. N. Sarazin, E. Morvan, M.A. di Forte Poisson, M. Oualli, C. Gaquière, O. Jardel, O. Drisse, M. Tordjman, M. Magis, and S. L. Delage, *IEEE Elec. Dev. Lett*. **31**(1), 11 (2010).
4. J. Kuzmik, G. Pozzovivo, C. Ostermaier, G. Strasser, D. Pogany, E. Gornik, J.-F. Carlin, M. Gonschorek, E. Feltin, and N. Grandjean, *J. Appl. Phys.* **106**(12), 124503 (2009).

5. T. Roy, Y.S. Puzyrev, B.R. Tuttle, D.M. Fleetwood, R.D. Schrimpf, D.F. Brown, U.K. Mishra, and S.T. Pantelides, *Appl. Phys. Lett.* **96**(13), 133503 (2010).
6. Y.S. Puzyrev, T. Roy, M. Beck, B.R. Tuttle, R.D. Schrimpf, D.M. Fleetwood, and S.T. Pantelides, *J. Appl. Phys.* **109**(3), 034501 (2011).
7. E. Bahat-Treidel, O. Hilt, F. Brunner, J. Würfl, and G. Tränkle, *IEEE Trans. Elec. Dev.* **55**(12), 3354 (2008).
8. A. Vescan, H. Hardtdegen, N. Ketteniß, M. Eickelkamp, A. Noculak, J. Goliasch, M.v.d. Ahe, H.L. Bay, T. Schäpers, H. Kalisch, D. Grützmacher, and R.H. Jansen, *Phys. Stat. Solidi (c)* **6**(2), S1003 (2009).
9. D.S. Lee, X. Gao, S. Guo, and T. Palacios, *IEEE Elec. Dev. Lett.* **32**(5), 617 (2011).
10. J. Kuzmik, S. Vitanov, C. Dua, J.-F. Carlin, C. Ostermaier, A. Alexewicz, G. Strasser, D. Pogany, E. Gornik, N. Grandjean, S. Delage, and V. Palankovski, *Jpn. J. Appl. Phys.* **51**, 054102 (2012).
11. S. Vitanov, V. Palankovski, S. Murad, T. Roedle, R. Quay, and S. Selberherr, *IEEE Tran. Elec. Dev.* **59**(3), 685 (2012).
12. A.F. Wright, *J. Appl. Phys.* **90**(3), 1164 (2001).